Electronic Supplementary Material (ESI) for CrystEngComm.

Spontaneous formation of hierarchical structures in some polylactide/polysilsesquioxane blends.

Supporting Information

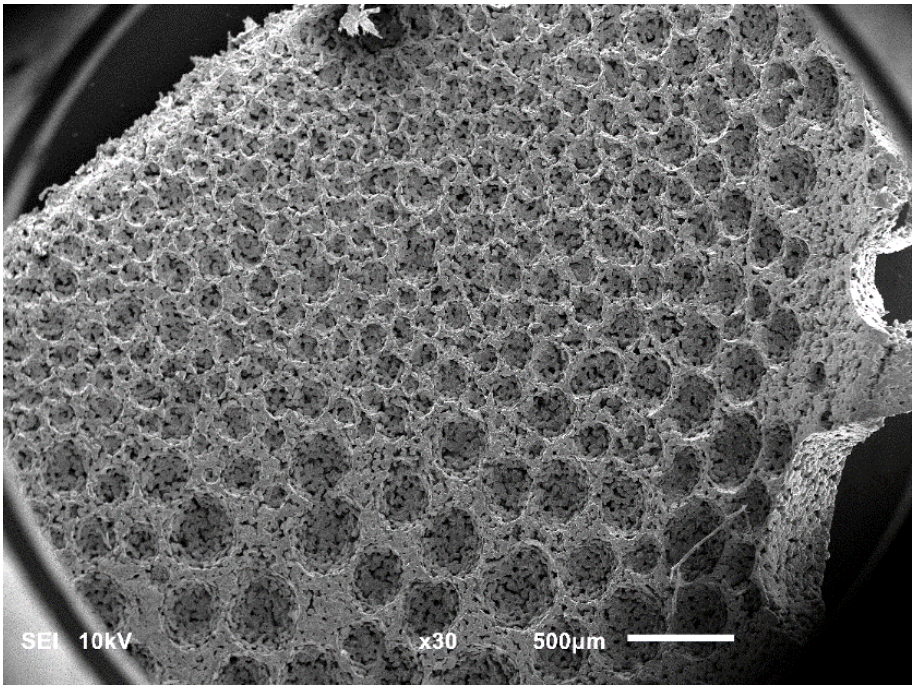

Figure S1. SEM micrograph of P/100-OH.

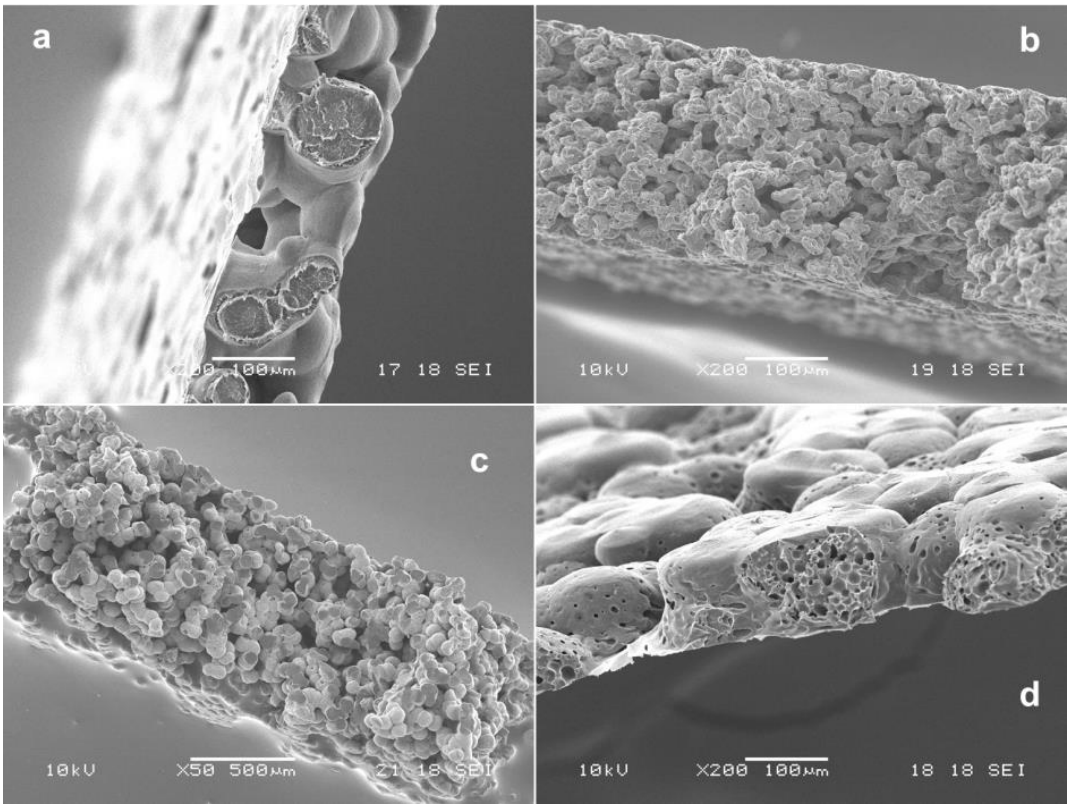

Figure S2. Freeze-fractured cross-sections of PLA (a), P/100-OH (b), P/100-COOH (c) and P/100-COOMe (d).

(a)

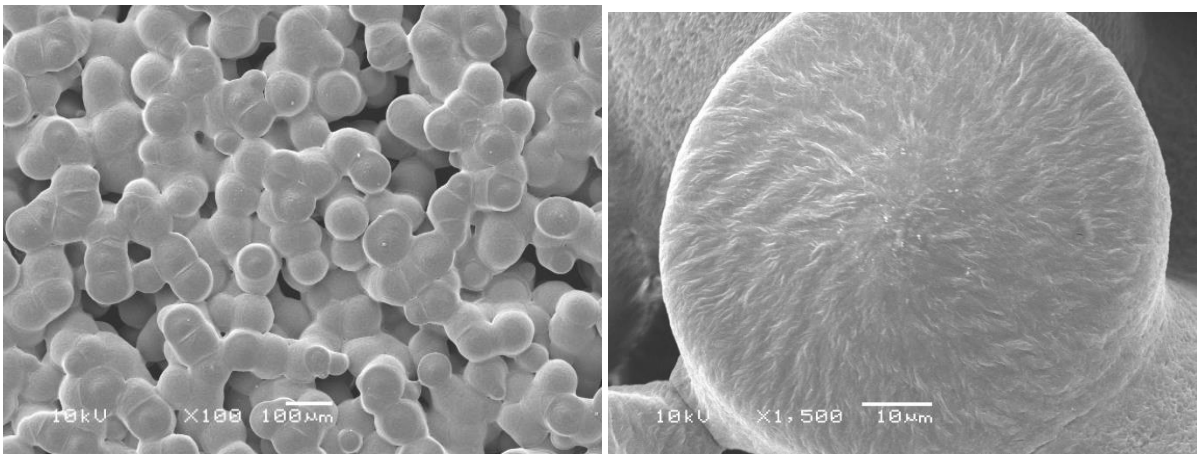

(b)

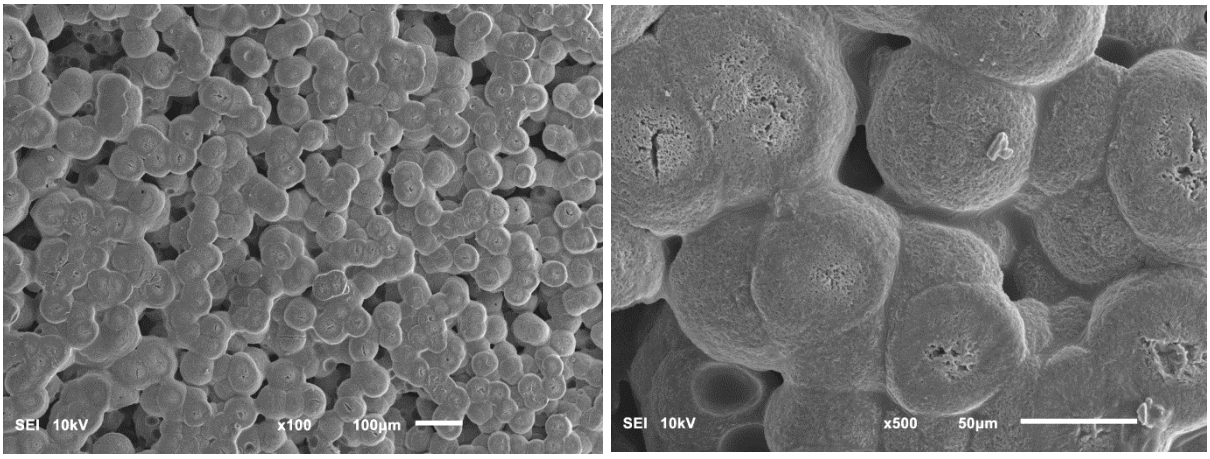

(c)

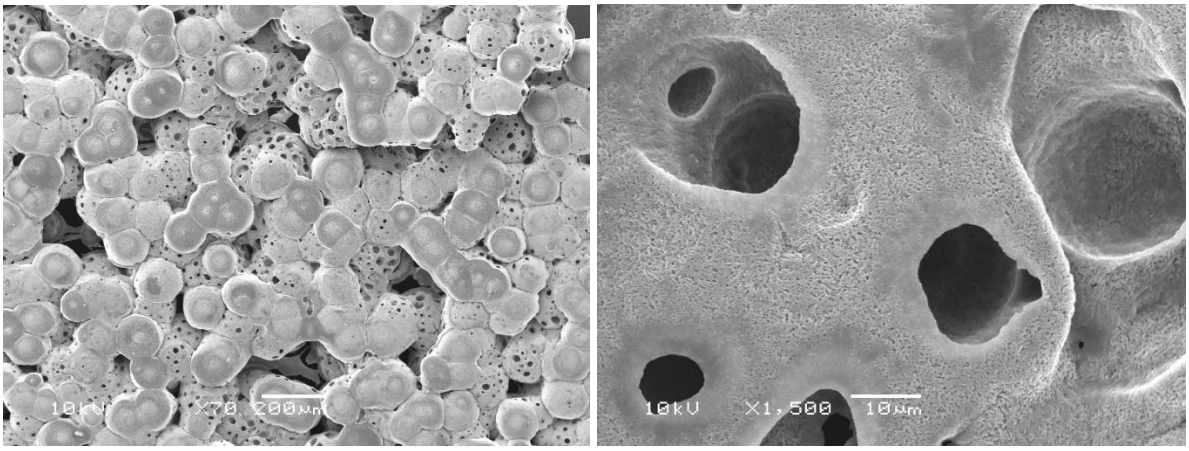

Figure S3. SEM micrographs of free surfaces of samples etched with MeOH (a) PLA THF; (b) P/100-COOH; (c) P/100-COOMe.

Table S1. Characteristic IR vibration modes (cm^{-1}) and Raman shifts (cm^{-1}) in PLA and LPSQ-R.

sample	spectroscopy	Characteristic modes
LPSQ-OH	IR	v(O-H) 3300; v(C-H) 2950-2850; δ_{β}(COH) 1410; $\delta_{as}(CH_2)$ 1409; v(C-O) 1277; δ_s(Si-CH_3) 1254; δ(Si-CH_2) 1180; v_{as}(Si-O) 1123; v_s(Si-O)1065, 1026; v(O-H) 944; v(Si-C) 758
	Raman	δ(COH) 1465; $\delta_{as}(CH_2)$ 1413; ρ(CH_2) 1177; v(CCO) in 1° alcohols 1003; v(CCO) in 1° alcohols 944; v(C-S) 763, 715, 659
LPSQ-COOH	IR	v(O-H) 3300; v(C-H) 2900-2650; v(C=O) 1700; δ_{β}(COH) 1414; $\delta_{as}(CH_2)$ 1409; v(C-O) 1282; δ_s(Si-CH_2) 1253; δ(Si-CH_2) 1181; v_{as}(Si-O) 1123; v_s(Si-O) 1095, 1040; v(O-H) 842; v(Si-C) 780
	Raman	v(C=O) 1700; δ(COH) 1440; $\delta_{as}(CH_2)$ 1406; ρ(CH_2) 1180; v(C-COO) 891; v(C-S) 789; 712; 672
LPSQ-COOMe	IR	v(C-H) 2950-2900; v(C=O) 1734; $\delta_{as}(CH_2)$ 1436; v(C-O) 1283; δ_s(Si-CH_2) 1254; δ(Si-CH_2) 1182; v_{as}(Si-O) 1127; v_s(Si-O) 1046; v(Si-C) 800
	Raman	v(C=O) 1731; $\delta_{as}(CH_2)$ 1411; ρ(CH_2) 1182; v(C-COO) 876; v(C-COO) 902; v(C-S) 789, 709
PLA	IR	v(C=O) 1760; δ_2CH 1304; v_{as}(COC)+δ(CH) 1270; v_{as}(COC)+ $\rho_{as}(CH_3)$ 1213, 1183, 1222 (cryst.), 1202 (cryst.); $\rho_s(CH_3)$ 1132, 1144 (cryst.); v_s(COC) 1081, 1093 (cryst.); v(C-CH_3) 1042, 1023; ρ(CH_3)+v(C-COO) amorphous 955; ρ(CH_3)+v(C-COO) (cryst.) 920-922; v(C-COO) 864; δC=O 740-760
	Raman	v(C=O) 1767; $\delta_{as}CH_3$ 1452; δ_sCH_3 1384; δ_1CH + δ_sCH_3 1349; δ_2CH 1298; δ(CH) + v(COC) 1220; v_{as}(COC) + $r_{as}CH_3$ 1180; $r_{as}CH_3$ 1126; v_s(COC) 1090; r(C-CH_3) 1042; $r$$CH_3$ + vCC 950; v(C-COO) 873

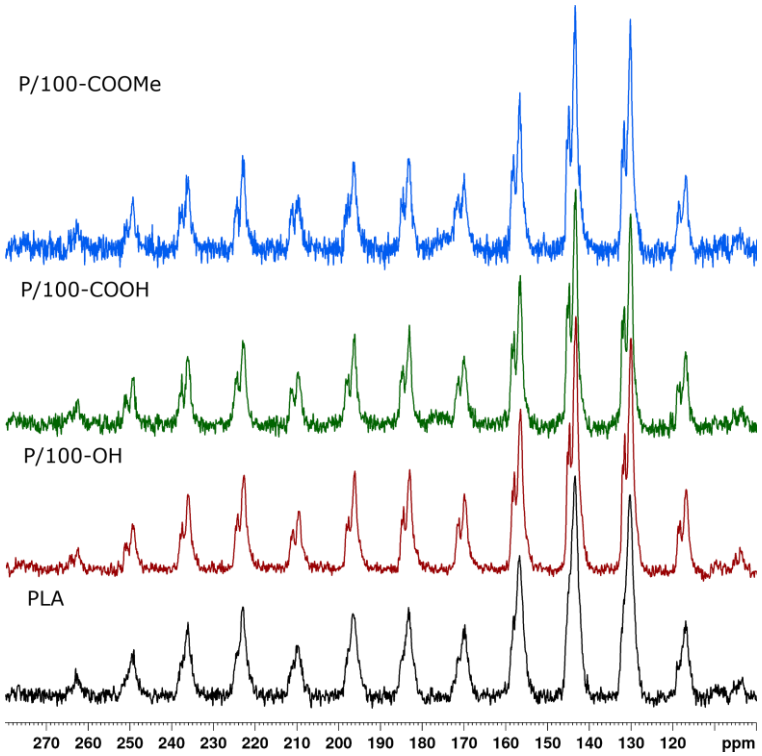

Figure S4. The shape of the ^{13}C chemical shielding tensors of carbonyl groups originating form pure PLA and P/100-R samples.

Table S2. Theoretical values of the isotropic and anisotropic ^{13}C shieldings arising from carbonyl group of a fragment of PLA molecule not interacting with any other molecules, as well as of the same fragment interacting via formation of C=O…H-O hydrogen bond with fragments of LPSQ-OH and LPSQ-COOH.

<table>
<tr><td colspan="2">PLA</td></tr>
<tr><td colspan="2"> 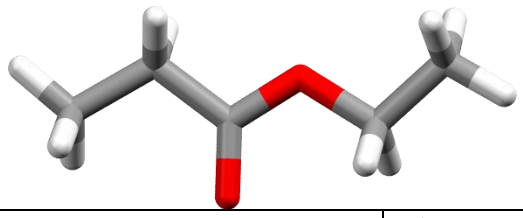
σ_{iso} = 2.8
σ_{11} = -95.4
σ_{22} = 38.2
σ_{33} = 65.6</td></tr>
<tr><td>P/100-OH</td><td>P/100-COOH</td></tr>
<tr><td> 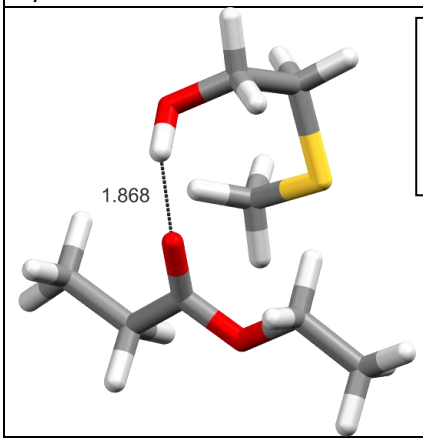

σ_{iso} = -1.0
σ_{11} = -93.4
σ_{22} = 20.1
σ_{33} = 70.3</td><td> 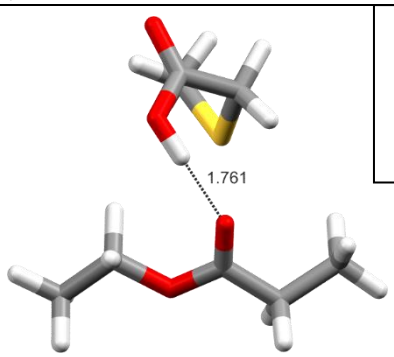

σ_{iso} = -2.6
σ_{11} = -89.4
σ_{22} = 10.2
σ_{33} = 71.3</td></tr>
</table>

Table S3. SCF energy and Gibbs free energy differences (in kJ/mol) between three conformations of 10-units chains of PLLA and PLLA+D.

starting conformation	SCF		ΔG	
	PLLA	PLLA+D	PLLA	PLLA+D
gt	0.00	0.00	0.00	0.00
gg	36.91	40.77	39.35	42.79
tg	84.73	44.00	88.40	56.66